Gravity and Magnetic Signatures of Tidal Flow in Ganymede's Ocean

Daoud Laariara[1,3], Jérémy Rekier[2,3], Tim Van Hoolst[3,4], and Véronique Dehant[2,3]

[1] Institute of Mechanics, Materials and Civil Engineering, Université Catholique de Louvain (UCLouvain), Louvain-la-Neuve, Belgium [2] Earth and Life Institute, UCLouvain, Louvain-la-Neuve, Belgium [3] Royal Observatory of Belgium, Brussels, Belgium [4] Instituut voor Sterrenkunde, KULeuven, Belgium

UCLouvain — ORB - KSB — fnrs LA LIBERTÉ DE CHERCHER

Motivation

- **Ganymede has a subsurface ocean** as supported by several evidences including magnetic measurements from Galileo and Juno[a], and auroral observations from the Hubble Space Telescope[b].
- **Jupiter's tides can drive periodic flows within the ocean.**
- **Tidal flows can induce signals** which are in principle observable. On Earth, satellites can measure the magnetic signature of ocean tidal flows[c].
- **Juice is on its way to Ganymede !** The low-altitude orbital phases of the mission (GCO500 and GCO200)[d,e] could make it possible to detect very weak signals.
- **Detection of tidal flows signatures can lead to a better understanding of Ganymede's ocean dynamics and to additional constraints on the moon's interior.**

Question

Can Juice detect the signatures in magnetic and gravity fields induced by Jupiter's eccentricity and obliquity tides, and how could such detections improve constraints on Ganymede's interior ?

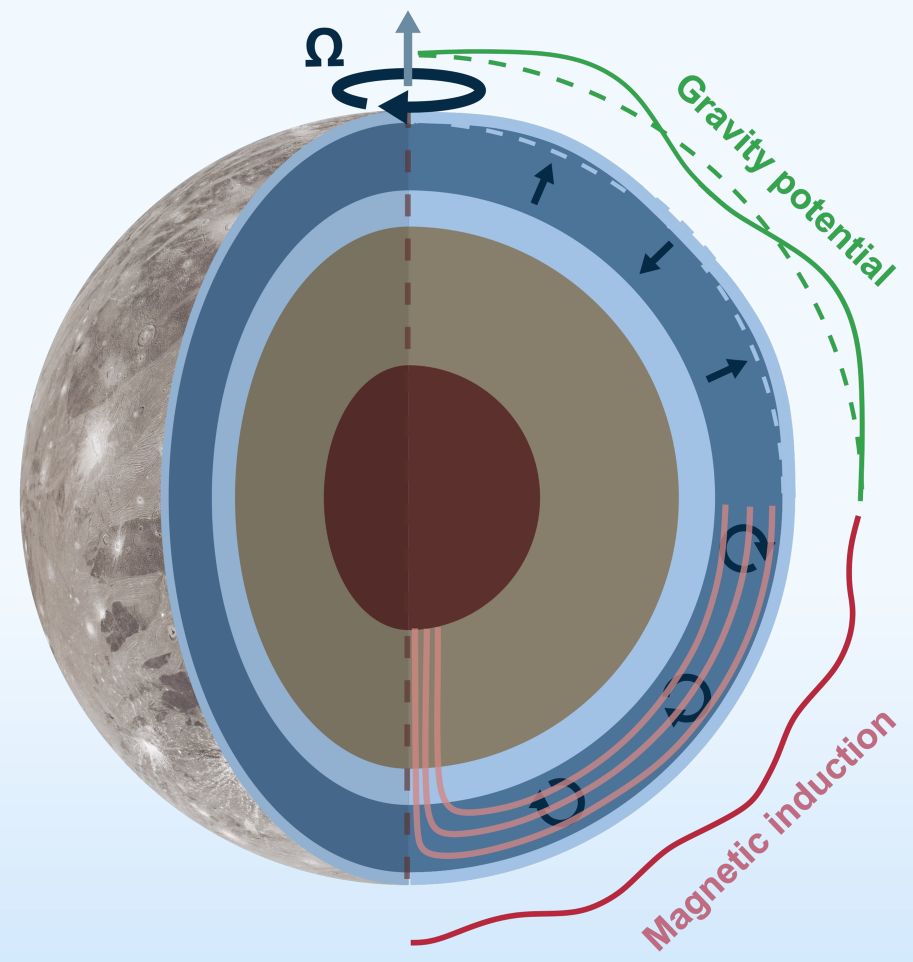

Summary

Conclusion

Flow

- Tides can excite resonant internal inertial waves within the ocean.
- Hitting a resonance can amplify the response enough to make the flow turbulent.
- Westward obliquity tide excite a resonant Rossby mode. Other tides can hit a resonance depending on the ocean geometry.

Signatures

- Signatures of eccentricity tides appear too small to be detected by Juice.
- Both **magnetic and gravitational signatures of the westward obliquity tide exceed the resolution of Juice's instruments** for a certain range of parameters.
- Although the intensity of the signals are above the resolution of the instruments, separation from ambient gravity and magnetic fields remains challenging.

Characterization

- **Successful detection can give additional constraints on ocean depth, ice shell thickness, ocean conductivity and effective viscosity.**

Future studies

To overcome the main limitations of the present work, future studies should:

- Include nonlinearities and a better handling of turbulence.
- Dynamically couple the ocean flow with the elasto-gravitational deformation of the moon in a geometry that is not perfectly spherical.
- Explore the coupling with other forcing mechanisms such as convection.

Method

Deformation

Step 1. Jupiter's tides deform Ganymede

- **Method:** we solve the classical **elasto-gravitational equations**[f] to compute degree 2 static tidal **Love numbers.**
- **Model and Assumptions:**
  - 5-layer interior model of Ganymede.
  - Homogeneous, non-rotating, and incompressible layers.
  - Perfectly elastic solid layers and inviscid liquid layers.
- **Output : Radial deformation** at the top of the ocean $\xi = h_2 \dfrac{\Phi_T}{g_0}$

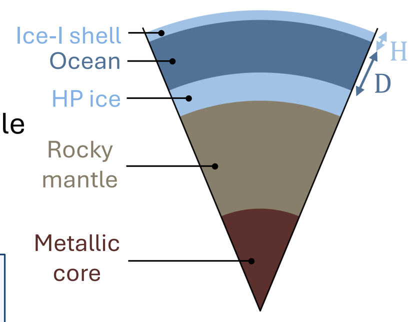

Eccentricity $(m = 0)$ — Obliquity $(m = 1)$ — Eccentricity $(m = 2)$

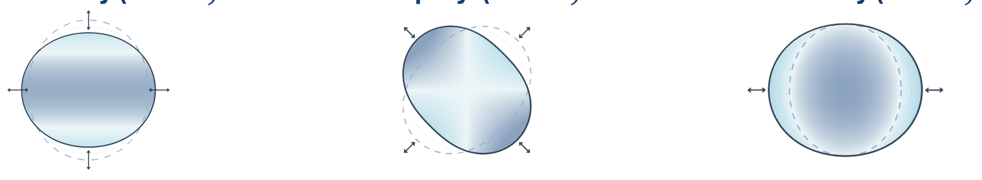

$\xi(E/W) =$ $1.3\,m$ — $0.4\,m$ / $0.4\,m$ — $3.8\,m$ / $0.5\,m$

Tidal flow

Step 2. The periodic deformation drives the flow

- **Method:** we solve the **linearized Navier-Stokes equations** in the ocean by imposing the displacement at the interface computed in Step 1 as **radial boundary forcing.**
- **Model and Assumptions:**
  - Perfectly spherical shell model of the ocean.
  - Newtonian, homogeneous, rotating and incompressible fluid.
  - Molecular Ekman number $\mathrm{Ek} = \upsilon/\Omega R^2 \sim 10^{-14}$.
  - **Linearization** : Rossby number $\mathrm{Ro} = U/\Omega R \ll 1$.

$$i\omega\,\mathbf{u} + 2\,\mathbf{e}_z \times \mathbf{u} = -\nabla p + \mathrm{Ek}\,\nabla^2 \mathbf{u}$$
$$\mathbf{u}(r = R) = i\,\Omega\,\xi_{\mathrm{tides}}$$

- **Numerical implementation:**
  - Spectral solver : **Kore.**
  - Orders m are decoupled $(m = 0,1,2)$.
  - Numerically accessible Ekman number up to $\mathbf{Ek = 10^{-10}}$.
  - Aspect ratio $\eta = (R - D)/R \in [0.8 - 0.99]$.
- **Tidal flow:**
  - Tides can excite linear internal **inertial modes**[g,h].
  - Inertial modes have frequencies $\boldsymbol{\omega} \in [\mathbf{-2\Omega - 2\Omega}]$.
  - Characterized by intense **shear layers.**

Signatures

Step 3. The tidal flow induce signals in gravity and magnetic fields

1) Magnetic field

- Motion of a conductive ocean $(\sigma \in [0.1 - 5]\ S/m)$ in a background magnetic field **induce a secondary magnetic field.**
- **Linearized induction equation** with insulating BC

$$i\omega\,\mathbf{b} = \nabla\times(\mathbf{u}\times\mathbf{B}_0) + \mathrm{Em}\,\nabla^2\mathbf{b}$$

with $\mathrm{Em} = 1/\mu_0\sigma\Omega R^2$

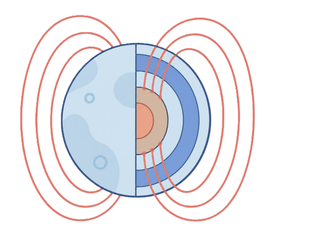

Ganymede's intrinsic dipolar field

$$\mathbf{B}_0 = \nabla\times\nabla\times\left[\frac{B_0}{2r^2}\,Y_1^0(\theta,\varphi)\,\mathbf{r}\right]$$

- Extrapolation towards **Juice GCO200** altitude.

2) Gravity field

- Global **elasto-gravitational deformations** due to **pressure field variations** associated with tidal flows at the ice-ocean interface.
- **Pressure Love numbers**[i] computed from the elasto-gravitational equations with the 5-layer Ganymede model.

$$\Phi^p_{\ell m} = -\frac{k^p_\ell}{\bar{\rho}}\,P_{\ell m}$$

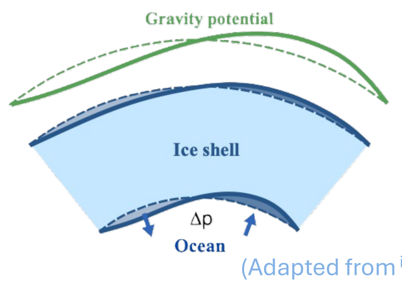

(Adapted from[i])

Results and Discussion

Eccentricity tides

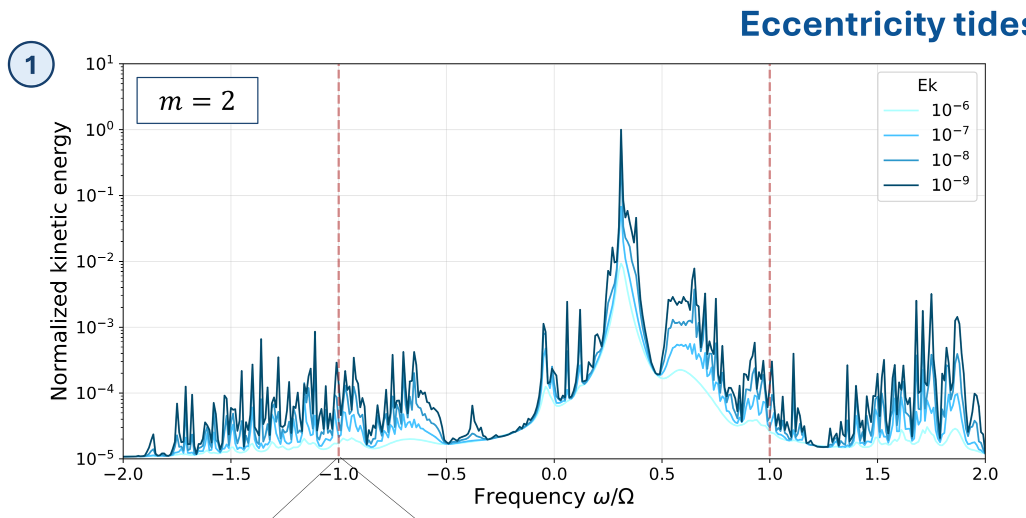

1. Frequency spectrum of the response

- $m = 2$ forcing ($m = 0$ not shown but equivalent).
- Spiky due to **inertial modes** excitation.
- Eccentricity tides at diurnal frequency $(\omega = \pm\,\Omega)$.

2. Spectrum of the prograde eccentricity tide

- Inertial modes excitation if the aspect ratio is **resonant.**
- Resonance amplify the flow intensity.
- Amplification increase with decreasing Ek. Shear layers become thinner and more intense.

3. Reynolds number

- If the amplification is sufficient, the flow may become **turbulent**. We compute the **Reynolds number** and extrapolate towards molecular Ek to assess the fluid regime (chosen critical value : 10^3).

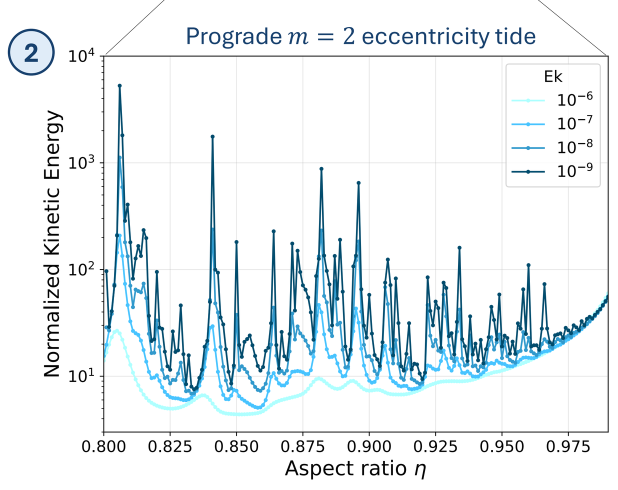

$\mathrm{Re} = \mathrm{Ro}\,\mathrm{Ek}^{-1/2}$

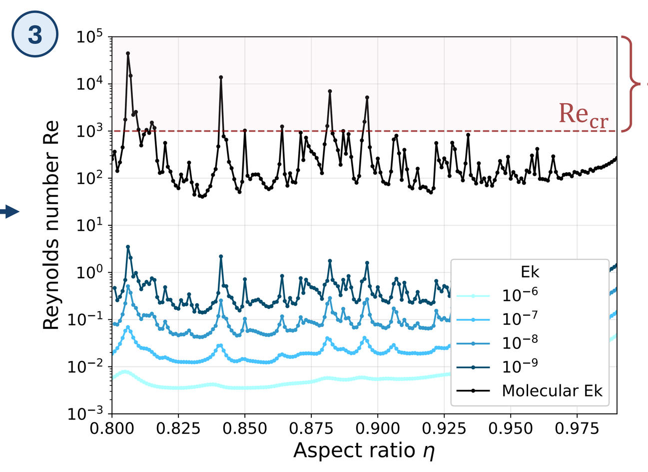

The flow becomes turbulent

- Linearity assumption breaks
- Turbulence modelled by an effective viscosity
- $\mathrm{Ek}^{\mathrm{eff}} \in [10^{-4} - 10^{-10}]$ to account for the uncertainty

4. Signatures

- Magnetic and gravity signatures of tidal flows compared to Juice's instruments expected accuracy
- Chosen mode $\eta = 0.806$ (Other modes are not shown but the conclusion remain identical).
- The presence of small-scale flow structure associated with shear layers lead to high-degree components
- Shaded area shows signal intensity variability with effective viscosity, ice shell thickness, ocean depth and ocean conductivity
- **Signal intensity remain below the detectability threshold for the entire parameter space**

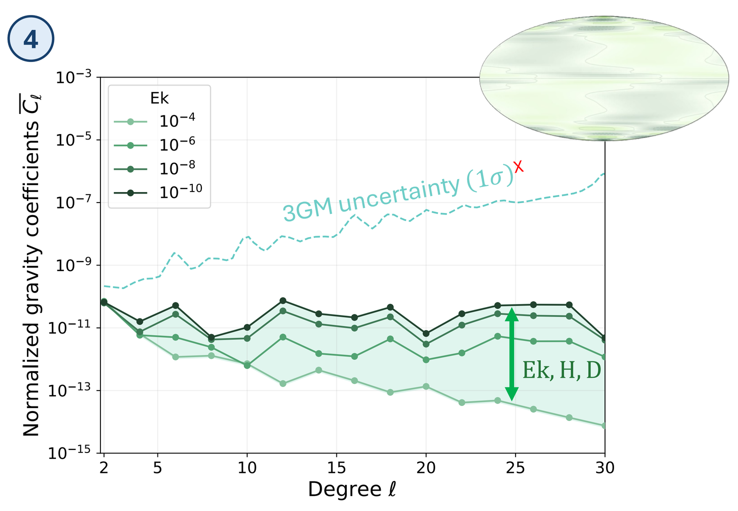

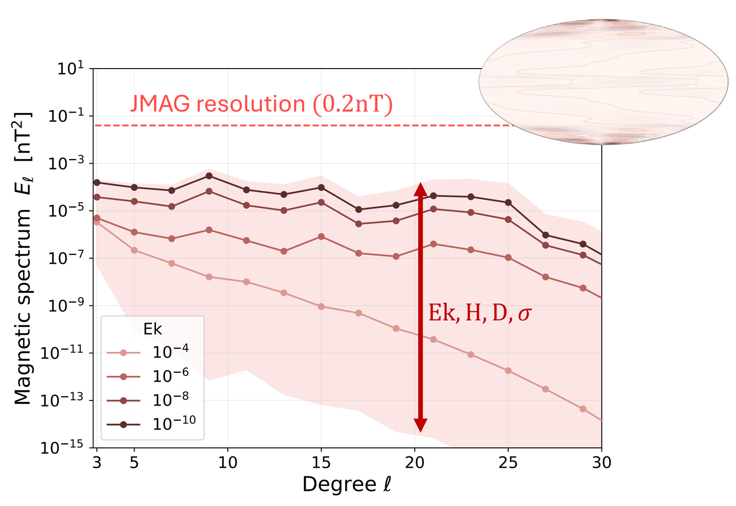

Undetectable signals

- Both magnetic and gravity signatures remain below the resolution of Juice's instruments
- Signals associated with eccentricity tides appear too weak to be detected

Obliquity tide

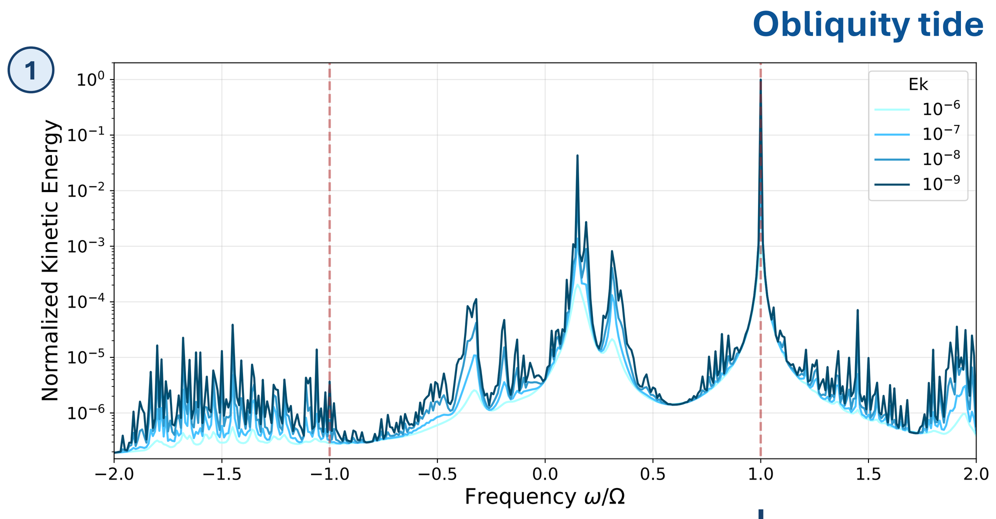

1. Frequency spectrum of the response

- $m = 1$ forcing
- Spiky due to **inertial modes** excitation.
- Large resonance at $\omega = \Omega$: spin-over mode
- **Spin-over mode:** Analogous to the purely toroidal Rossby-Haurwitz mode of degree and order 1[j].
- **The westward obliquity tide excite the spin-over mode**

2. Reynolds number

- Resonant amplification of the flow intensity. The Rossby number scales as $\mathrm{Ek}^{-1/2}$ reflecting that the response is dominated by **Ekman layers** (whose thickness scales as $\mathrm{Ek}^{1/2}$). Consequently, the Reynolds number scales as Ek^{-1}
- Extrapolation towards molecular Ek show that the flow becomes **turbulent**

$\mathrm{Re} = \mathrm{Ro}\,\mathrm{Ek}^{-1/2}$

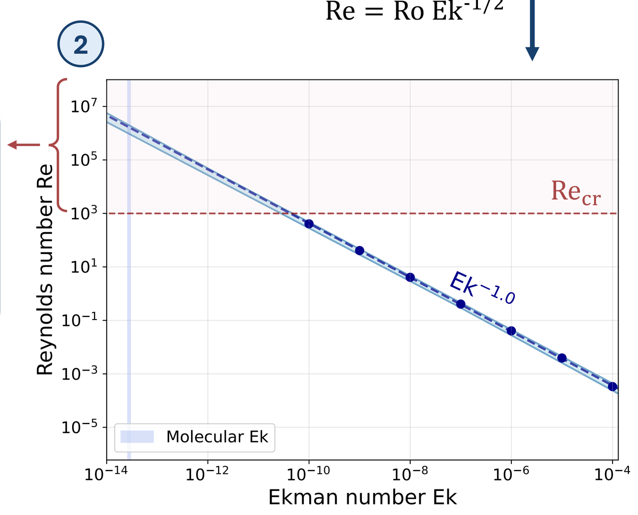

3. Signatures

- Signatures associated with the spin-over are of low-degree
  - The gravity signal is mainly of degree 2.
  - The magnetic signal is mainly of degree 1 (dipolar).
- The intensity of the signals scales as $\mathrm{Ek}^{-1/2}$, just like Ro.
- For a certain range of parameters, **the signals exceed the resolution** of the instruments.

4. Characterization

- Dependence of the signals intensity to Ganymede's physical parameters. Shown for $\mathrm{Ek} = 10^{-9}$.
- A successful detection can lead to **additional constraints on Ganymede's interior,** both from intensity and phase information (not shown).

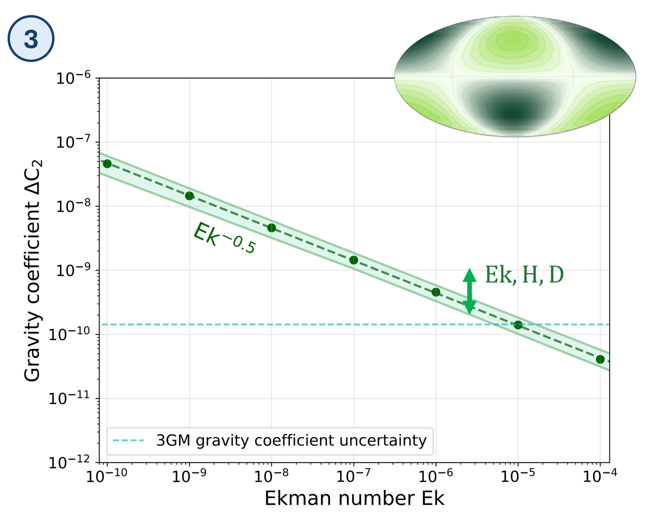

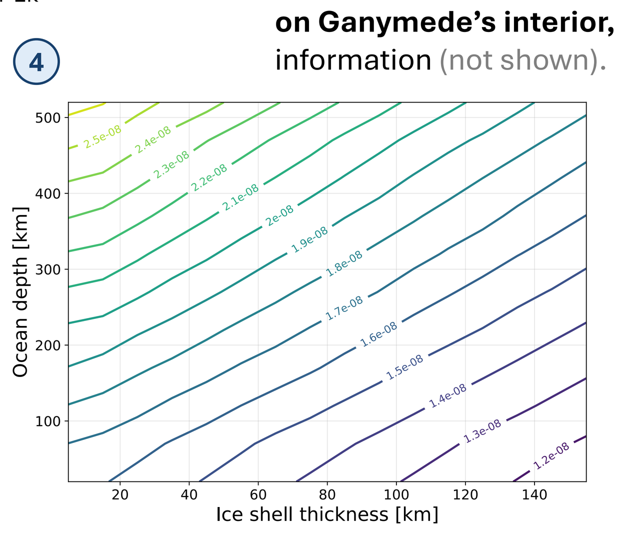

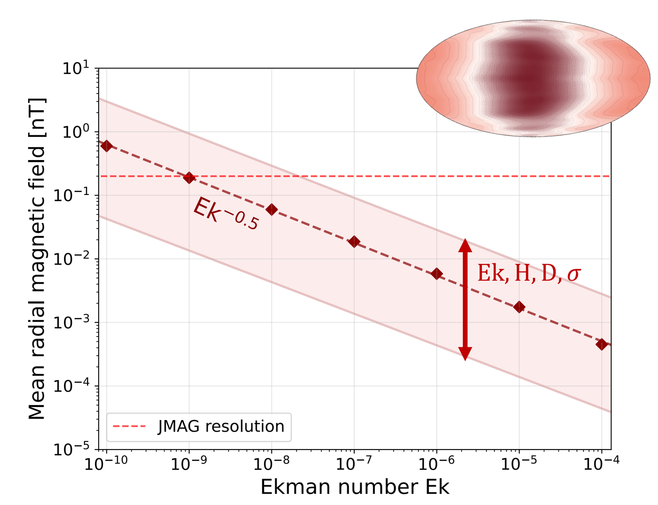

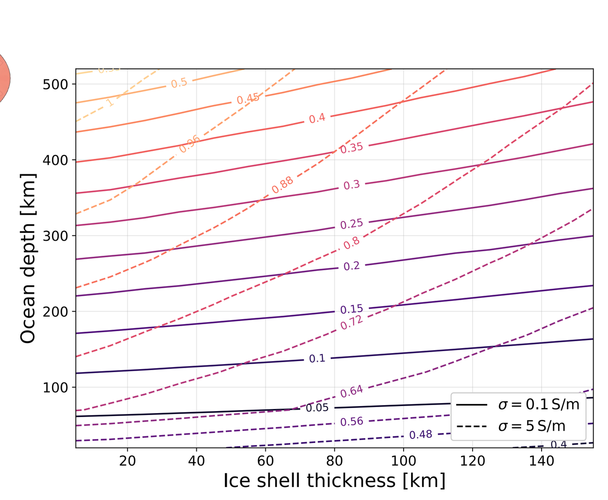

Detectable signals

- Both gravity and magnetic signatures appear possibly detectable.
- Intensities at $\mathrm{Ek} = 10^{-10}$ must be taken as upper bounds
- Successful detection gives constraints on Ganymede's interior
- Detection is challenging as the low-degree signals must be separated from the ambient fields.
- Limitation: the perfect frequency match between the mode and the tide could be affected in a not-perfectly spherical geometry[k].
- Limitation: the constant effective viscosity turbulence model is overly simplistic.

References

[a] Kivelson, M. G., Khurana, K. K., Russell, C. T., Walker, R. J., Warnecke, J., Coroniti, F. V., et al. (1996). Nature, 384(6609), 537–541.
[b] Saur, J., Duling, S., Roth, L., Jia, X., Strobel, D. F., Feldman, P. D., et al. (2015). Journal of Geophysical Research: Space Physics, 120(3), 1715–1737.
[c] Grayver, A., Finlay, C. C., & Olsen, N. (2024). Philosophical Transactions of the Royal Society A, 382(2286), 20240078.
[d] Boutonnet, A., Langevin, Y., Erd, C. (2024). Space Science Reviews 220, 67.
[e] Van Hoolst, T., Tobie, G., Vallat, C., Altobelli, N., Bruzzone, L., Cao, et al. (2024). Space Science Reviews 220, 54.
[f] Dahlen, F.A., Tromp, J. (1998). Theoretical global seismology. Princeton University Press, Princeton, N.J.
[g] Rekier, J., Trinh, A., Triana, S.A., Dehant, V. (2019a). Geophysical Journal International 216, 777–793.
[h] Rovira-Navarro, M., Rieutord, M., Gerkema, T., Maas, L.R., van der Wal, W., Vermeersen, B. (2019). Icarus 321, 126–140.
[i] Dumberry, M., Bloxham, J. (2004). Geophysical Journal International 159, 417–434.
[j] Tyler, R.H. (2008). Nature 456, 770–772
[k] Rovira-Navarro, M., Gerkema, T., Maas, L.R., Van Der Wal, W., Van Ostayen, R., Vermeersen, B. (2020). Icarus 343, 113711.

Acknowledgements

D. Laariara is a Research Fellow of the Fonds de la Recherche Scientifique – FNRS. Computational resources have been provided by the Consortium des Équipements de Calcul Intensif (CÉCI), funded by the Fonds de la Recherche Scientifique de Belgique (F.R.S.-FNRS) under Grant No. 2.5020.11 and by the Walloon Region

Abstract information